THE JOURNAL OF BIOLOGICAL CHEMISTRY VOL. 287, NO. 22, pp. 17930–17941, May 25, 2012
© 2012 by The American Society for Biochemistry and Molecular Biology, Inc. Published in the U.S.A.

Excision of *Trpv6* Gene Leads to Severe Defects in Epididymal Ca^{2+} Absorption and Male Fertility Much Like Single D541A Pore Mutation*[S]

Received for publication, November 28, 2011, and in revised form, February 20, 2012 Published, JBC Papers in Press, March 15, 2012, DOI 10.1074/jbc.M111.328286

Petra Weissgerber[‡1], Ulrich Kriebs[‡1], Volodymyr Tsvilovskyy[‡§1], Jenny Olausson[‡], Oliver Kretz[¶], Christof Stoerger[‡], Stefanie Mannebach[‡], Ulrich Wissenbach[‡], Rudi Vennekens[‡], Ralf Middendorff[‖], Veit Flockerzi[‡], and Marc Freichel[‡§2]

From the [‡]Experimentelle und Klinische Pharmakologie und Toxikologie, Universitaet des Saarlandes, 66421 Homburg, Germany, [‖]Institut für Anatomie und Zellbiologie, Justus Liebig Universitaet Giessen, Aulweg 123, 35385 Giessen, Germany, [¶]Zentrum für Neurowissenschaften, Universitaet Freiburg, Albertstrasse 23, 79104 Freiburg, Germany, and [§]Pharmakologisches Institut, Universitaet Heidelberg, Im Neuenheimer Feld 366, 69120 Heidelberg, Germany

Background: The $TRPV6^{D541A}$ pore mutation abrogates epididymal Ca^{2+} absorption causing hypofertility in mice, raising the possibility of residual $TRPV6^{D541A}$ channel activity.
Results: *Trpv6* deletion reduces fertility parameters to the same extent as the D541A pore mutation.
Conclusion: The D541A pore mutation leads to complete inactivation of TRPV6 channels in epididymal epithelium.
Significance: Targeted mutations in mice help to understand the function of TRPV6 proteins in native systems.

Replacement of aspartate residue 541 by alanine (D541A) in the pore of TRPV6 channels in mice disrupts Ca^{2+} absorption by the epididymal epithelium, resulting in abnormally high Ca^{2+} concentrations in epididymal luminal fluid and in a dramatic but incomplete loss of sperm motility and fertilization capacity, raising the possibility of residual activity of channels formed by $TRPV6^{D541A}$ proteins (Weissgerber, P., Kriebs, U., Tsvilovskyy, V., Olausson, J., Kretz, O., Stoerger, C., Vennekens, R., Wissenbach, U., Middendorff, R., Flockerzi, V., and Freichel, M. (2011) *Sci. Signal.* 4, ra27). It is known from other cation channels that introducing pore mutations even if they largely affect their conductivity and permeability can evoke considerably different phenotypes compared with the deletion of the corresponding protein. Therefore, we generated TRPV6-deficient mice ($Trpv6^{-/-}$) by deleting exons encoding transmembrane domains with the pore-forming region and the complete cytosolic C terminus harboring binding sites for TRPV6-associated proteins that regulate its activity and plasma membrane anchoring. Using this strategy, we aimed to determine whether the $TRPV6^{D541A}$ pore mutant still contributes to residual channel activity and/or channel-independent functions *in vivo*. $Trpv6^{-/-}$ males reveal severe defects in fertility and motility and viability of sperm and a significant increase in epididymal luminal Ca^{2+} concentration that is mirrored by a lack of Ca^{2+} uptake by the epididymal epithelium. Therewith, *Trpv6* excision affects epididymal Ca^{2+} handling and male fertility to the same extent as the introduction of the D541A pore mutation, arguing against residual functions of the $TRPV6^{D541A}$ pore mutant in epididymal epithelial cells.

The maintenance of body Ca^{2+} homeostasis is essential for many vital functions including neuronal excitability, muscle contraction, and bone formation. Ca^{2+} acquisition in the body occurs via trans- and paracellular transport processes across the continuous layer of epithelial cells. About 10 years ago, transcripts of the structurally closely related TRPV6 and TRPV5 were identified in the epithelia of the kidney (2), in the duodenum (3), and in placenta, pancreatic acinar cells, and other exocrine glands (4–7), and expression of the *Trpv6* and *Trpv5* cDNAs in HEK293 cells or other expression systems leads to the formation of cation channels with a high selectivity for Ca^{2+} (3–5, 8). These channels exhibit many features possessed by Ca^{2+} transporters in epithelial cells (6, 7): they mediate passive transport of Ca^{2+} down the electrochemical gradient without energy consumption, and they are constitutively active (4, 5, 8). Accordingly, they were assumed to be epithelial Ca^{2+} uptake channels.

Crucial for Ca^{2+} permeation through TRPV6 and TRPV5 channels is a single aspartate residue within the pore-forming loop of both proteins; replacing this aspartate residue at position 541 in mouse TRPV6 or at position 542 in rabbit TRPV5 by an alanine residue renders the channels impermeable to Ca^{2+} (9). We studied the impact of this mutation *in vivo* with a mouse model in which the D541A mutation of TRPV6 was introduced in the germ line by a gene targeting approach (1). Males homozygous for this single amino acid substitution ($TRPV6^{D541A/D541A}$) exhibited a severely impaired fertility and a large reduction of motility and fertilization capacity of sperm despite intact spermatogenesis. An increase in Ca^{2+} in spermatozoa is an important signal to promote their

* This work was supported by the Deutsche Forschungsgemeinschaft (to M. F., V. F., P. W., and R. M.), Fonds der Chemischen Industrie and Sander-Stiftung (to V. F.), LOEWE program (to R. M.), and Landes-Offensive zur Entwicklung Wissenschaftlich-ökonomischer Exzellenz (LOEWE), Homburger Forschungsförderungsprogramm (HOMFOR) and Forschungsausschuss der Universität des Saarlandes (to M. F., V. F., P. W., and V. T.).
[S] This article contains supplemental Movies S1 and S2.
[1] These authors contributed equally to this work.
[2] To whom correspondence should be addressed: Pharmakologisches Inst., Universitaet Heidelberg, Im Neuenheimer Feld 366, 69120 Heidelberg, Germany. Tel.: 49-6221-5486861; E-mail: marc.freichel@pharma.uni-heidelberg.de.

motility, capacitation, and the acrosome reaction (10, 11), but *Trpv6* transcripts were not detectable in spermatozoa or in the germinal epithelium, and there was no evidence for a cell-autonomous impairment of sperm Ca^{2+} signaling (1). However, we identified *Trpv6* transcripts in the epididymal epithelium and TRPV6 proteins in the apical membrane of this epithelium and showed that the luminal Ca^{2+} concentration is increased by 10-fold in the caudal epididymal fluid of $Trpv6^{D541A/D541A}$ males compared with that of wild-type mice. Additional measurements of Ca^{2+} uptake from the epididymal fluid from $Trpv6^{D541A/D541A}$ mice into the epididymis revealed a reduction of uptake by 7–8-fold compared with fluid from wild-type animals (1). Apparently, the intact TRPV6 proteins are essential components of Ca^{2+} uptake channels in the epididymal epithelium that are responsible for the decrease of the Ca^{2+} concentration in the epididymal fluid along the epididymal duct, generating a luminal Ca^{2+} gradient with higher Ca^{2+} concentration in the caput portion (proximal segments) of the epididymal duct and lower Ca^{2+} concentrations in its caudal (distal) segments. It is well known that the composition of the epididymal fluid differs considerably among separate epididymal segments. This is caused by differences in secretory and absorptive activities of the epididymal epithelium (12–16), resulting in changes of the net water; the HCO_3^- reabsorption; the secretion of proteins; concentrations of Na^+, Cl^-, and K^+; and luminal acidification. Notably, the Ca^{2+} concentration decreases markedly in the epididymal fluid along the epididymal duct toward its distal segments, the cauda epididymis (14). It is this luminal Ca^{2+} gradient that is severely compromised by the $TRPV6^{D541A}$ mutation, resulting in a dramatic but incomplete loss of sperm motility and fertilization capacity.

The direct electrophysiological recording of channel activity was not possible either from wild-type or from D541A mutant epididymal cells. Our own results and a survey of the literature on TRPV6 and its closest relative, TRPV5, revealed that direct recordings of TRPV6 and TRPV5 currents from acutely prepared primary cells expressing *Trpv6* or *Trpv5* transcripts have not been described. Instead, Ca^{2+} uptake measurements similar to those we performed (17) have been used to identify (10, 18) and characterize these channels in primary cells. Although Ca^{2+} uptake was reduced by 7–8-fold in $Trpv6^{D541A/D541A}$ mice, we could not exclude residual channel activity of the properly expressed and trafficked, yet mutated $TRPV6^{D541A}$ proteins, which might in addition serve channel-independent functions as structural and/or scaffolding components (19) of the epithelial plasma membrane. Thus, the $TRPV6^{D541A}$ mutation might not be sufficient to identify all TRPV6-related functions, and it is conceivable that a complete loss of TRPV6 proteins leads to additional phenotypes. Similarly, the $GluR\delta2^{Q618R}$ pore mutation, although rendering GluRδ2 channels nominally impermeable to Ca^{2+} (20), did not cause the defects in synaptic plasticity of hippocampal neurons and motor coordination that were evoked by the complete inactivation of the GluRδ2 gene in mice (21). We therefore generated a second mouse line using a Cre-loxP-based gene targeting strategy to delete exons 13, 14, and 15 of the *Trpv6* gene that encode part of the fifth and sixth transmembrane-spanning domains, the pore linker in between, and the complete cytosolic C terminus. By deleting almost one-third of the protein-encoding DNA, we not only eliminated an essential part of the ion-conducting pore but also disrupted essentially the predicted structure of the protein. We now show that mice homozygous for this gene excision were viable, and our analysis reveals that the Ca^{2+} concentration in the caudal epididymal fluid and the motility, fertilization capacity, and viability of $Trpv6^{-/-}$ sperm are affected to the same extent as in $Trpv6^{D541A/D541A}$ mice. These results indicate that the TRPV6 deletion occurring in $Trpv6^{-/-}$ mice does not further aggravate the phenotype observed in $Trpv6^{D541A/D541A}$ mice, arguing against residual channel activity and against channel-independent scaffolding functions of the $TRPV6^{D541A}$ protein that may influence epididymal Ca^{2+} absorption or fertilization capacity indirectly.

EXPERIMENTAL PROCEDURES

All animal experiments were performed in accordance with German legislation on the protection of animals and were approved by the local ethics committee. The generation of $TRPV6^{-/-}$ mice and the maintenance of the mouse line as well as the experiments performed were approved (reference number K110/180-07; approved on December 10, 2002, December 28, 2004, and January 17, 2007) by the "Kreispolizeibehörde des Saarpfalz-Kreises, Deutschland" and was performed by M. F., V. F., P. W., U. K., J. O., S. B., K. F., and C. M. All these people got permission to perform the experiments described by the local ethics committee and "Kreispolizeibehörde des Saarpfalz-Kreises, Deutschland." They all have a long-standing experience and authorization in the generation and phenotypic analysis of transgenic mice (*e.g.* Ref. 1 and references therein).

Generation of TRPV6 Knock-out Mice—The 5′ and 3′ homology arms of the targeting vector were amplified from genomic DNA of R1 ES cells using *Pfu* polymerase. The 5′ homology arm was cloned 5′ of a loxP site followed by the genomic sequence containing exons 13, 14, and 15; an FRT[3] sequence-flanked PGK promotor-driven neomycin resistance gene cassette (neo), and a second loxP site. The sequence of the loxP site was inserted in the 16th intron of the *Ephb6* gene, which is oriented tail to tail with *Trpv6* in the mouse genome separated by 120 bp only. Accordingly, Cre-mediated excision of exons 13, 14, and 15 of the *Trpv6* gene leads to deletion of exons 17 and 18 of the adjacent *Ephb6* gene. The herpes simplex virus thymidine kinase cassette (HSVtk) and an eGFP cassette were introduced for negative selection. Gene targeting in R1 ES cells was performed as described (1). One of 327 double resistant colonies showed homologous recombination at the *Trpv6* locus as confirmed by Southern blot hybridization with a 5′ and 3′ probe external to the targeting vector and a neo probe. Germ line chimeras were obtained by injection of correctly targeted ES cell clone 6F11 into C57Bl/6 blastocysts. $Trpv6^{-/-}$ mice on the mixed (129/SvJ × C57Bl/6N) background were compared with F1 offspring of 129SvJ × C57Bl/6N matings unless stated otherwise. Routinely, mice were genotyped using PCR. Additionally, an independent $Trpv6^{-/-}$ mouse line was generated from

[3] The abbreviation used are: FRT, Flp recombinase target site; PGK, phosphoglycerol kinase.

Trpv6$^{+/D541A}$ mice (ES cell clone 8E11b) by Cre-mediated excision of genomic sequences containing exons 13–15 and analyzed via computer-assisted sperm analysis. All animal experiments were performed according to the Guide for the Care and Use of Laboratory Animals published by the United States National Institutes of Health and were approved by the local ethics committee.

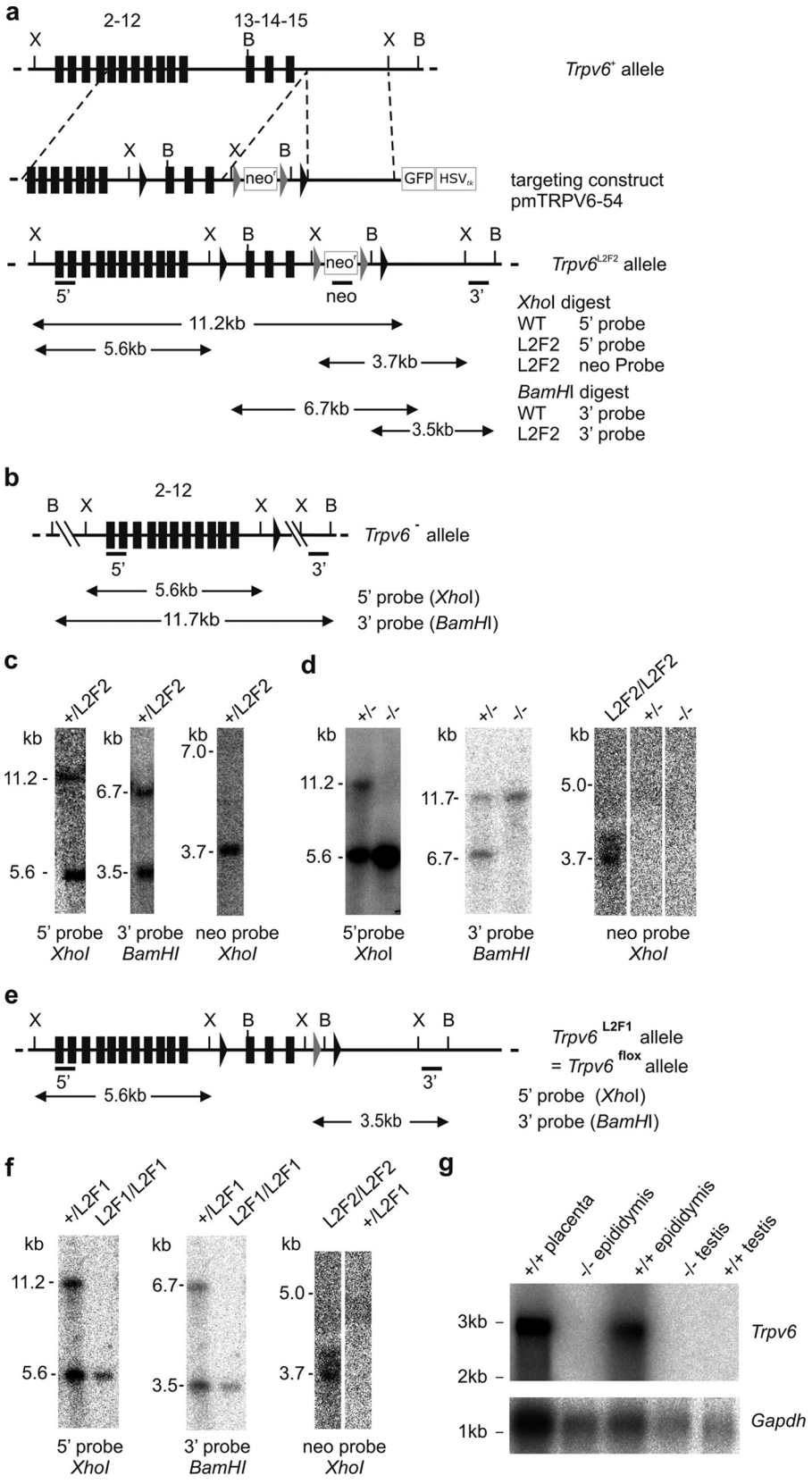

Expression Analysis of Trpv6-encoding Transcripts—Poly-$(A)^+$ RNA (10 μg) from epididymis and testis of wild-type and $Trpv6^{-/-}$ mice was used for Northern blot analysis as described (17). Blots were hybridized with a randomly labeled cDNA probe comprising exons 13, 14, and 15 of the m*Trpv6* cDNA (nucleotides 1741–2849; GenBank™ accession number AJ542487), and filters were exposed to x-ray films for 19 h. To analyze expression of *Trpv6* transcripts in prostate, we prepared RNA from prostate using the RNeasy Mini kit (Qiagen) and performed one-step reverse transcription-PCR (RT-PCR; Invitrogen) using 20 ng of total RNA/reaction. The following intron-spanning primers were used: for amplification of a specific *Trpv6* fragment comprising 258 bp: UK_V6_16 (5′-GTC TGG CAT CAG CCT CAG C-3′; exon 1) and UK_V6_33 (5′-CTC ACA TCC TTC AAA CTT GAG C-3′; exon 2); for amplification of full-length *Trpv6* cDNA comprising 2312 bp: UK_V6_17 (5′-CAG GGT CGA GCC CAG TTG G-3′; located in the 5′-untranslated region of exon 1) and UK_V6_14 (5′-CTC GCA GGA TGA CCT TAG CTG-3′; located in the 3′-untranslated region of exon 15). RNA isolated from epididymis was used as a positive control.

Mating, Weight Gain, and Fertility Analysis—Fertility analysis was done basically as described in Weissgerber *et al.* (1). In brief, adult male $Trpv6^{+/-}$ and $Trpv6^{-/-}$ mice were continuously housed with adult $Trpv6^{+/-}$ and $Trpv6^{-/-}$ females over a period of 16 weeks, and the number and size of litters as well as the genotype of offspring were recorded. Considering 3 weeks per pregnancy and assuming that the adult female mouse gets pregnant within the 1st week after the birth of the litter, four litters can be expected per mating under optimal conditions during this time period of 16 weeks. In reality, we observed that each wild-type/wild-type mating produced slightly fewer numbers of litters, that is 3.375 litters in 16 weeks (27 litters per eight matings; see Ref. 1). All mating analyses described in this study and by Weissgerber *et al.* (1) were performed in our animal facility under identical conditions. For copulatory behavior analysis, the ratio of plug-positive females per mating was evaluated. After flushing of the oviduct of plug-positive females, collected embryos were distinguished from non-fertilized eggs by Hoechst 33258 staining of DNA. Body weight was analyzed weekly in wild-type, $Trpv6^{+/-}$, and $Trpv6^{-/-}$ littermates from $Trpv6^{+/-}$ intercrosses until the age of 21 weeks. To compare body weight development between $Trpv6^{-/-}$ and $Trpv6^{D541A/D541A}$ mice, body weight at the age of 4, 8, 12, and 16 weeks was divided by the body weight of the same mouse at the age of 1 week and normalized to the corresponding body weight ratio obtained from wild-type littermates. Isolation of spermatozoa, computer-assisted sperm analysis, *in vitro* fertilization, and sperm viability analysis were performed as described in detail (1).

Analysis of Segregation of the $Trpv6^-$ Allele—To analyze whether the $Trpv6^-$ allele was inherited in a mendelian ratio, $Trpv6^{+/-}$ males and females at the age of 3–4 months were intercrossed, and offspring were analyzed with respect to the *Trpv6* genotype.

Videomicroscopic Analysis of Sperm Motility—Capacitated spermatozoa were placed in a 100-μm chamber at 37 °C temperature on a slide warmer and videotaped using a DCR-SR90 Handycam (Sony) connected to an inverted microscope (AxioVision 40 CFL, Zeiss). Selected sequences were processed using Adobe PREMIERE software.

Miscellaneous Methods—Whole organ preparation, histological analysis, and Ca^{2+} measurements in the epididymal fluid were done as described (1).

Statistical Analysis—Data are presented as mean ± S.E. of *n* independent experiments unless otherwise stated. The Origin 7.0 software (OriginLab) was used for statistical analysis. Significance was assessed with the two-sample Student's *t* test ($p < 0.05$ for significance) unless stated otherwise. Offspring frequency in the mating analysis and weight gain were analyzed using analysis of variance. The occurrence of different genotypes in the inheritance analysis of the $Trpv6^-$ allele was analyzed using a two-tailed χ^2 test (GraphPad Software).

RESULTS

Generation and Characterization of $Trpv6^{-/-}$ Mice—We used a Cre-loxP-mediated gene targeting strategy in embryonic stem cells to generate *Trpv6*-deficient mice (Fig. 1, *a* and *b*). We confirmed homologous recombination in $Trpv6^{+/L2F2}$ ES cells and Cre-mediated excision of exons 13, 14, and 15, which encode part of transmembrane domain 5, transmembrane domain 6, the pore-forming region in between, and the adjacent amino acids forming the complete intracellular C terminus of TRPV6, in $Trpv6^{+/-}$ and $Trpv6^{-/-}$ mice by Southern blot analysis (Fig. 1, *c* and *d*). In parallel, mice heterozygous for the $Trpv6^{L2F2}$ allele ($Trpv6^{+/L2F2}$) were bred with FlpeR (129S4/SvJaeSor-Gt (ROSA)26Sortm1(FLP1) Dym/J) mice (18) to remove the neo^r cassette and to produce mice with a conditional $Trpv6^{+/L2F1}$ allele (Fig. 1, *e* and *f*). Northern blot analysis revealed specific 2.9-kb *Trpv6* transcripts expressed in placenta

FIGURE 1. **Targeted deletion of TRPV6 channel pore and C terminus.** We used a Cre-loxP strategy to excise exons 13, 14, and 15, which encode the pore region, part of the fifth and the entire sixth transmembrane-spanning domains, and the cytosolic C terminus of TRPV6. *a*, the wild-type $Trpv6^+$ allele, targeting construct, and recombinant $Trpv6^{L2F2}$ allele. Translated exons (not in scale) are shown as *filled boxes*. In the $Trpv6^{L2F2}$ allele, exons 13, 14, and 15 are flanked by loxP sites (*filled triangles*). An FRT site (*gray triangles*)-flanked PGK-neo^r cassette is located upstream of the second loxP site. *B*, BamHI; *X*, XhoI. Probes and sizes of genomic DNA fragments as expected by Southern blots are indicated. *HSVtk*, herpes simplex virus thymidin kinase. *b*, Cre-mediated conversion of the $Trpv6^{L2F2}$ allele to the $Trpv6^{-/-}$ allele in mice. *c*, identification of the recombinant $Trpv6^{L2F2}$ allele in recombinant ES cells by Southern blot analysis using 5′ and 3′ probes placed externally to the targeted sequence and a neo probe that is directed against the internal PGK-neo^r cassette. *d*, Cre-mediated generation of the $Trpv6^{-/-}$ allele in mice resulted in the conversion of the 3.5-kb fragment of the $Trpv6^{L2F2}$ allele to an 11.7-kb fragment (3′ probe; BamHI digest). The 5′ probe and XhoI digestion produce a 5.6-kb fragment for the $Trpv6^-$ allele. In addition, Cre activity also leads to the excision of the PGK-neo^r cassette so that the 3.7-kb neo probe signal detectable for the $Trpv6^{L2F2}$ allele is absent in $Trpv6^{+/-}$ and $Trpv6^{-/-}$ animals (neo probe; XhoI digest). *e* and *f*, Flp-mediated generation of the $Trpv6^{L2F1}$ allele in mice produces a 5.6-kb fragment (5′ probe; XhoI digestion) and a 3.5-kb fragment (3′ probe; BamHI digest) for the $Trpv6^{L2F1}$ allele. In addition, Flp activity also leads to the excision of the PGK-neo^r cassette so that the 3.7-kb neo probe signal detectable for the $Trpv6^{L2F2}$ allele is absent in $Trpv6^{L2F1}$ animals (neo probe; XhoI digest). *g*, Northern blot analysis of poly$(A)^+$ RNA isolated from placenta from wild-type (+/+) mice and from epididymis and testis from wild-type (+/+) and $Trpv6^{-/-}$ (−/−) mice hybridized with m*Trpv6*-specific probe). 2.9-kb transcripts were identified in wild-type placenta and epididymis. No signal was detected in wild-type testis or in epididymis and testis of $Trpv6^{-/-}$ mice. *Gapdh* was used as a loading control.

a

total number of pups: 477	+/+	+/-	-/-
numbers of genotypes	124	227	126
observed frequency (%)	26,0	47,59	26,41
expected frequency (%)	25	50	25
Chi-square	1,126		
p value	0,57		

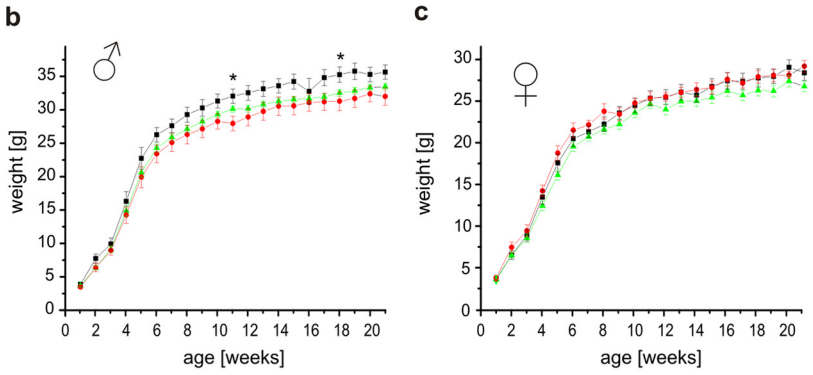

d

type	matings ♂	matings ♀	number of matings	mating time (weeks)	total number of offsping	litters per 16 weeks of mating	observed number of litters	expected number of litters
1	+/-	-/-	7	112	190	3.71	26	28
2	-/-	-/-	5	80	0	0.00 * $	0	20
3	-/-	+/-	9	144	6	0.33 * $	3	36
4	-/-	+/+	3	48	0	0.00 * $	0	12
5 §	+/+	+/+	8	128	183	3.375	27	32

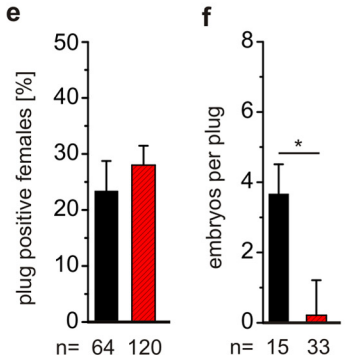

FIGURE 2. **Segregation of *Trpv6*$^{-}$ allele is normal, but *Trpv6*$^{-/-}$ males are hypofertile despite normal copulatory behavior.** *a*, segregation analysis from 477 offspring derived from 62 litters and 16 *Trpv6*$^{+/-}$ × *Trpv6*$^{+/-}$ matings. *b* and *c*, weight gain analysis in wild-type (*black*), *Trpv6*$^{+/-}$ (*green*), and *Trpv6*$^{-/-}$ (*red*) male (*b*) and female (*c*) mice. Body weight was recorded weekly between 1 and 21 weeks of age. Six to seven male and nine to 10 female wild-type mice, 19–27 male and 17–18 female *Trpv6*$^{+/-}$ mice, and nine male and six to seven female *Trpv6*$^{-/-}$ mice were analyzed. *, $p < 0.05$ *d*, offspring analysis from matings between wild-type (+/+), *Trpv6*$^{+/-}$ (+/−), and *Trpv6*$^{-/-}$ (−/−) mice. The number of matings, the cumulative mating time of all matings with mice of a given genotype, the total number of offspring, the ratio between the number of litters and number of matings, and the observed and expected number of litters are indicated. §, redrawn from Weissgerber *et al.* (1); *, $p < 0.001$ *versus* wild-type/wild-type matings and $p < 0.001$ *versus* male (♘) +/− × female (♀) −/− (type 1) matings; $, not statistically different: type 2 *versus* type 3 ($p = 0.17$) matings and type 3 *versus* type 4 ($p = 0.29$) matings. *e*, analysis of copulatory behavior by vaginal plug frequency in timed matings of wild-type (*black*) and *Trpv6*$^{-/-}$ (*red*) males with wild-type females. *n*, total number of analyzed matings; *, $p > 0.5$. *f*, averaged number of isolated embryos from matings with wild-type (*black*) and *Trpv6*$^{-/-}$ (*red*) males. *n*, numbers of analyzed vaginal plug-positive females; *, $p < 0.01$. Data are presented as mean ± S.E.

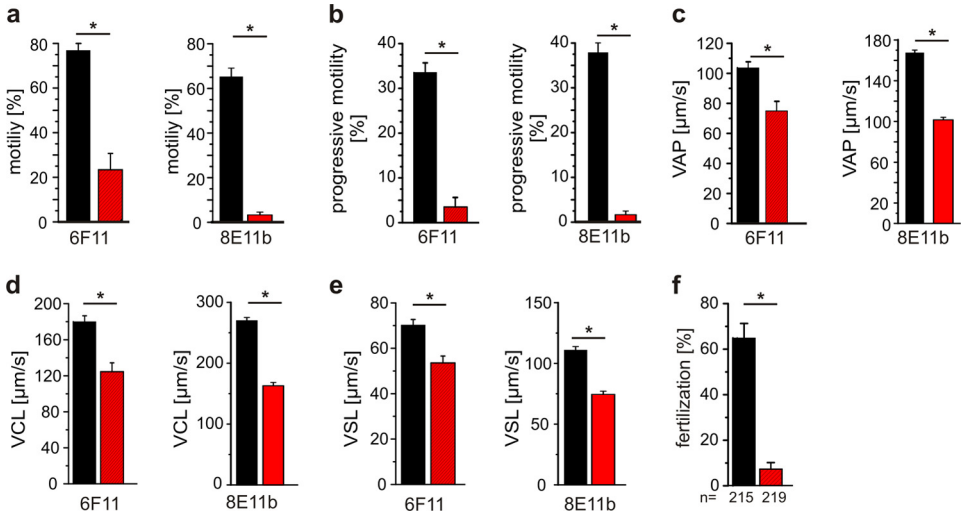

FIGURE 3. **Decreased motility and fertility of spermatozoa isolated from *Trpv6*$^{-/-}$ mice.** *a–e*, computer-assisted sperm analysis of sperm isolated from the cauda epididymis of *Trpv6*$^{-/-}$ mice (ES cell clone 6F11) and of an independent *Trpv6*$^{-/-}$ mouse line (ES cell clone 8E11b; generated from *Trpv6*$^{+/D541A}$ mice (1)). Average motility (*a*), progressive motility (*b*), path velocity (velocity average path (*VAP*)) (*c*), track velocity (velocity curvilinear (*VCL*)) (*d*), and linear velocity (velocity straight line (*VSL*)) (*e*) of spermatozoa from wild-type (*black*; $n = 8$) and *Trpv6*$^{-/-}$ (*red*; $n = 6$) mice 90 min after capacitation; *, $p < 0.001$. *f*, *in vitro* fertilization experiments. Averaged fraction of fertilized eggs incubated with spermatozoa from wild-type (*black*) and *Trpv6*$^{-/-}$ (*red*) mice; *, $p < 0.001$; *n* indicates the number of analyzed eggs. Data are presented as mean ± S.E.

and epididymis but not in testis from wild-type mice (Fig. 1*g*), supporting our previous finding that TRPV6 is not expressed in testes. After Cre-mediated excision, *Trpv6* transcripts were no longer detectable in epididymis of the resulting *Trpv6*$^{-/-}$ mice (Fig. 1*g*), confirming effective excision of the *Trpv6* gene. However, this lack of TRPV6 expression is in contrast to the results obtained from epididymis of *Trpv6*$^{D541A/D541A}$ mice where the identical probe hybridized to *Trpv6* transcripts indistinguishable from the transcripts observed in wild type (1). *Trpv6*$^{-/-}$ mice were viable and showed no obvious anatomical abnormalities, and the *Trpv6*$^{-}$ allele was segregated with the expected Mendelian frequency (Fig. 2*a*). Analysis of the weight gain of *Trpv6*$^{+/-}$ males and females revealed no growth defects during development and adulthood up to 21 weeks after birth (Fig. 2, *b* and *c*).

Trpv6 Gene Deletion Drastically Diminishes Male Fertility—Breeding analysis revealed that no offspring were born from intercrosses of *Trpv6*$^{-/-}$ mice in five independent matings (Fig. 2*d*). To assess whether the impaired reproduction was due to defects in male fertility similar to that in *Trpv6*$^{D541A/D541A}$ mice, we performed a systematic breeding analysis with mice of different genotypes. The results showed that *Trpv6*$^{-/-}$ males did not produce offspring with either *Trpv6*$^{-/-}$ females or *Trpv6*$^{+/+}$ females. In matings of male *Trpv6*$^{-/-}$ mice with female *Trpv6*$^{+/-}$ mice, only three litters with a total number of only six pups resulted from nine individual matings, whereas matings of male *Trpv6*$^{+/-}$ mice produced 26 litters with altogether 190 offspring in seven matings. The latter frequency corresponds to the frequency of offspring obtained after mating of wild-type mice (1). Apparently, the competence of *Trpv6*$^{-/-}$ males to fertilize females is considerably reduced. To rule out the possibility that *Trpv6*$^{-/-}$ males were not copulating, we performed timed matings of wild-type females with either wild-type or *Trpv6*$^{-/-}$ males (Fig. 2*e*). We counted the number of plug-positive females and determined that *Trpv6*$^{-/-}$ males exhibited normal copulatory behavior, but the number of successfully fertilized oocytes isolated from females impregnated with *Trpv6*$^{-/-}$ males was negligible compared with wild-type males (Fig. 2*f*). Accordingly, *Trpv6*$^{-/-}$ males recognized females and showed normal copulatory behavior but produced pregnancies and offspring with only minor success, indicating that *Trpv6* deletion leads to male hypofertility.

Impaired Motility and Fertilization Capacity of Sperm from Trpv6$^{-/-}$ *Mice*—Videomicroscopic analysis of capacitated sperm from wild-type mice (see supplemental Movie S1, wild-type sperm) indicated forceful beating and progressive movement. In contrast, most of the *Trpv6*$^{-/-}$ sperm were immotile with impaired movement and bending in the tail region (see supplemental Movie S2, *Trpv6*$^{-/-}$ sperm). Computer-assisted sperm analysis of capacitated sperm isolated from the cauda epididymis revealed that the number of motile sperm from *Trpv6*$^{-/-}$ mice (Fig. 3*a*) and their progressive motility were significantly decreased compared with sperm from wild-type mice (Fig. 3, *a* and *b*). Even within the small population of *Trpv6*-deficient sperm that showed progressive motility (Fig. 3, *c–e*), all speed parameters were significantly reduced, demonstrating that the *Trpv6* deletion critically affected sperm motility. The analysis of a second, independent *Trpv6*$^{-/-}$ mouse line, which we generated from the *Trpv6*$^{+/D541A}$ mice (1), confirmed these results (Fig. 3, *a–e*).

We performed *in vitro* fertilization experiments to analyze the ability of *Trpv6*$^{-/-}$ sperm to fertilize oocytes. Therefore, isolated mature eggs from wild-type females were incubated with capacitated wild-type or *Trpv6*$^{-/-}$ sperms, and the successful fertilization (indicated by the development of two-cell-stage embryos) was examined after 24 h. 161 of 238 eggs were fertilized by wild-type sperm, but only 18 of 265 eggs were fertilized by sperm derived from *Trpv6*$^{-/-}$ mice (Fig. 3*f*).

The reproductive tracts of wild-type and *Trpv6*$^{-/-}$ males were macroscopically examined and showed no obvious differences (Fig. 4*a*). No morphological differences were observed in histological sections of the testes from *Trpv6*$^{-/-}$ and wild-type

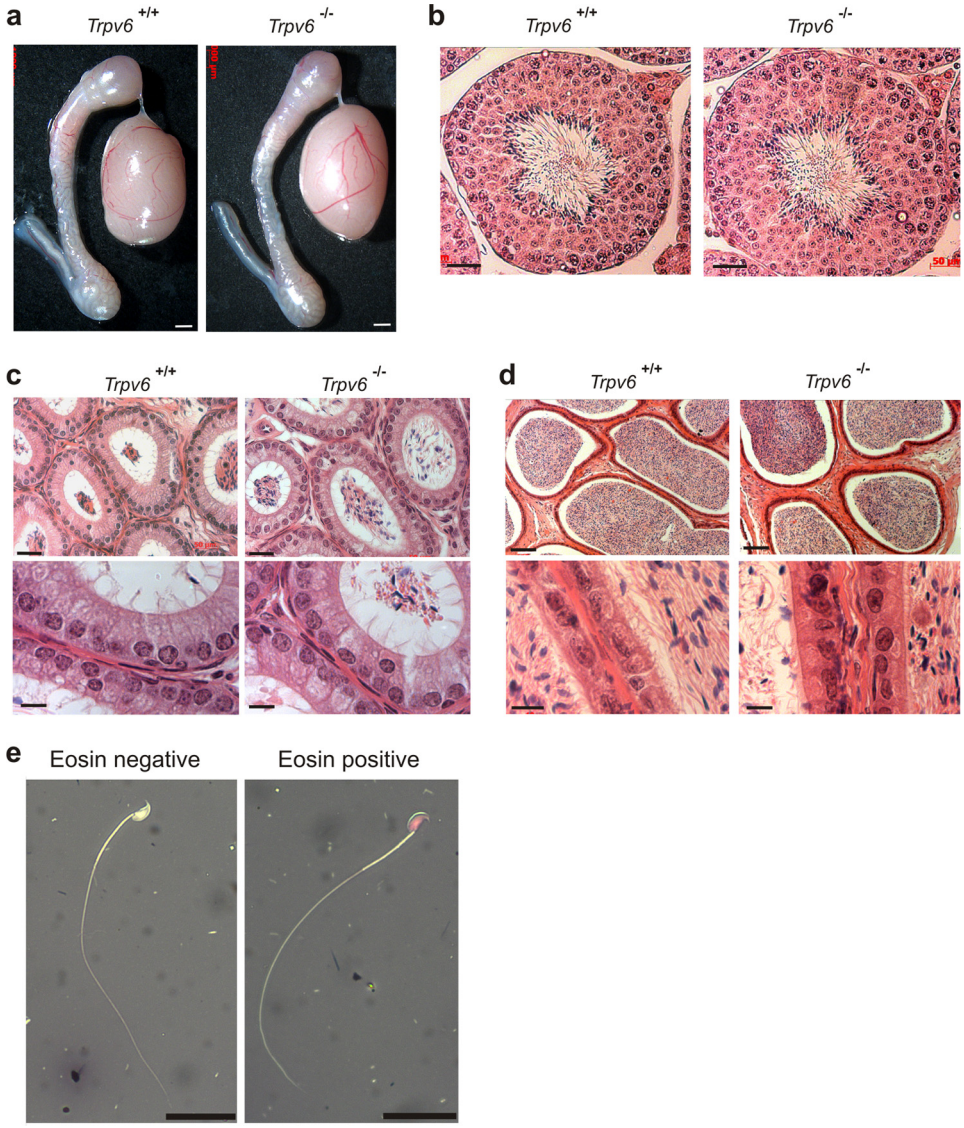

FIGURE 4. **Analysis of morphology of male reproductive organs and sperm viability in *Trpv6*$^{-/-}$ mice.** *a*, representative examples of whole mount preparations of reproductive organs from wild-type (+/+) and *Trpv6*$^{-/-}$ (−/−) mice. *Scale bar*, 1 mm. *b–d*, hematoxylin/eosin-stained sections of testis (*b*, *scale bar*, 50 μm), caput epididymis (*c*, *upper panels*, *scale bar*, 100 μm and *lower panels*, *scale bar*, 10 μm) and cauda epididymis (*d*, *upper panels*, *scale bar*, 100 μm and *lower panels*, *scale bar*, 10 μm) from wild-type (*Trpv6*$^{+/+}$) and *Trpv6*$^{-/-}$ mice. *e*, representative eosin/nigrosin stainings of vital (colorless sperm head; *left*) and dead spermatozoa (eosin-stained sperm head; *right*) isolated from cauda epididymis. *Scale bars*, 25 μm.

males (Fig. 4*b*); all cell types that can be observed during spermatogenesis, such as spermatogonia, spermatocytes, and spermatids, were apparent. In sections through the epididymis, we observed that the lumen of caput (Fig. 4*c*) and cauda (Fig. 4*d*) epididymis were filled with sperm. Additionally, microscopic analysis with higher magnification demonstrated that there were no differences between the morphology of the epididymal epithelium in *Trpv6*$^{-/-}$ and wild-type mice (Fig. 4, *c* and *d*, *lower panels*). Eosin-nigrosin staining of sperm (Fig. 4*e*) revealed that the number of viable *Trpv6*$^{-/-}$ sperm isolated from the caput epididymis was 62.53 ± 4.71% (1219 sperm analyzed from four mice) and from the cauda epididymis was 6.66 ± 2.84% (n = 4; 3003 sperm analyzed). In our previous study, we have shown that the reduction of the number of eosin-negative sperm during the epididymal passage was also more than 10-fold in *Trpv6*$^{D541A/D541A}$ mice but only 2-fold in wild-type mice (1).

As shown in Fig. 1*g*, *Trpv6* transcripts were not detectable in testes from wild-type mice. Also, no defects in spermatogenesis were observed in the testes of *Trpv6*$^{-/-}$ mice. Taken together, these results suggest (like in the *Trpv6*$^{D541A/D541A}$ mice) a secondary cause of the impaired viability of cauda epididymal sperm in *Trpv6*$^{-/-}$ mice. We have shown that the TRPV6 and TRPV6^{D541A} proteins are apparently expressed in the apical membrane of epididymal epithelial cells (1) and the lack of TRPV6 expression in epithelial cells from *Trpv6*$^{-/-}$ mice (see Fig. 1*g* and Ref. 1). A luminal Ca^{2+} gradient along the epididymal duct has been described (14) with luminal Ca^{2+} being lower in the cauda than in the caput, and we had found that luminal Ca^{2+} is markedly increased in the cauda from *Trpv6*$^{D541A/D541A}$ mice when compared with the Ca^{2+} levels in wild-type mice. Therefore, we analyzed whether the Ca^{2+} concentration of the intraluminal fluid in the cauda epididymis in *Trpv6*$^{-/-}$ mice is affected to the same extent using ion-selective microelectrodes.

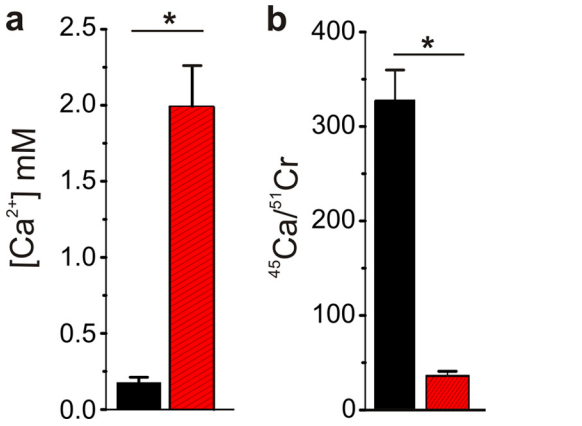

FIGURE 5. ***Trpv6*$^{-/-}$ mice exhibit excessively high Ca^{2+} concentration in epididymal fluid and show impaired epididymal Ca^{2+} uptake.** *a*, determination of the Ca^{2+} concentration in the cauda epididymal luminal fluid of wild-type (*black*) and *Trpv6*$^{-/-}$ (*red*) mice using ion-selective electrodes. The number of analyzed epididymides are as follows: wild-type, $n = 8$; *Trpv6*$^{-/-}$, $n = 8$; *, $p < 0.00001$. *b*, ratio of ^{45}Ca and ^{51}Cr-EDTA uptake in cauda epididymis of wild-type (*black*) ($n = 10$; five animals) and *Trpv6*$^{-/-}$ (*red*) ($n = 10$; five animals) mice. The ratio of $^{45}Ca/^{51}Cr$ activity accumulated in cauda epididymis was determined 30 min after intratubular administration of the isotopes; *, $p < 0.00001$. Data are presented as mean ± S.E.

Luminal fluids of the caudal epididymal duct contained ~11-fold higher concentrations of Ca^{2+} in *Trpv6*$^{-/-}$ mice (2.0 ± 0.3 mM; $n = 8$) compared with wild-type mice (0.18 ± 0.02 mM; $n = 8$; Fig. 5*a*). Next, we measured $^{45}Ca^{2+}$ uptake in the cauda epididymis. Fig. 5*b* shows a 9-fold decrease in the ratio of $^{45}Ca/^{51}Cr$ in the epididymis from *Trpv6*$^{-/-}$ mice compared with wild-type littermates, indicating a severe defect in Ca^{2+} absorption.

A higher luminal Ca^{2+} concentration may result in the formation of Ca^{2+} precipitates. Hence, alizarin red stainings of epididymal tissue sections were performed, but no Ca^{2+} depositions were recognized in epididymal sections (Fig. 6*a*). As we have shown previously (1, 5), TRPV6 is also expressed in the prostate (Fig. 6*c*). In contrast to the findings in the epididymis, the ventral, dorsal, and lateral lobes of the *Trpv6*$^{-/-}$ prostate (Fig. 6*b*, *lower panel*) showed Ca^{2+} depositions, and Ca^{2+} precipitates were macroscopically detectable as white rigidification (Fig. 6*b*, *upper panel*). The ducts were enlarged and showed a loss of epithelial infoldings into the lumen (Fig. 6*b*, *middle panel*).

DISCUSSION

In this study, we showed that deletion of part of the transmembrane domains including the pore-forming region and the entire C terminus of TRPV6 proteins led to hypofertility in *Trpv6*$^{-/-}$ males. A systematic breeding analysis revealed that the number of offspring in matings with homozygous *Trpv6*$^{-/-}$ males was markedly diminished regardless of the genotype of the females, whereas their copulatory behavior as well as the morphology of testis and epididymis was unaffected. However, the motility, fertilization capacity, and viability of sperm derived from cauda epididymis of *Trpv6*$^{-/-}$ males were drastically reduced; Ca^{2+} concentrations were abnormally high in the caudal fluid of *Trpv6*$^{-/-}$ males; and Ca^{2+} uptake by the epididymal epithelium was drastically impaired. Ca^{2+} precipitations were not identified in the epididymis but were found in

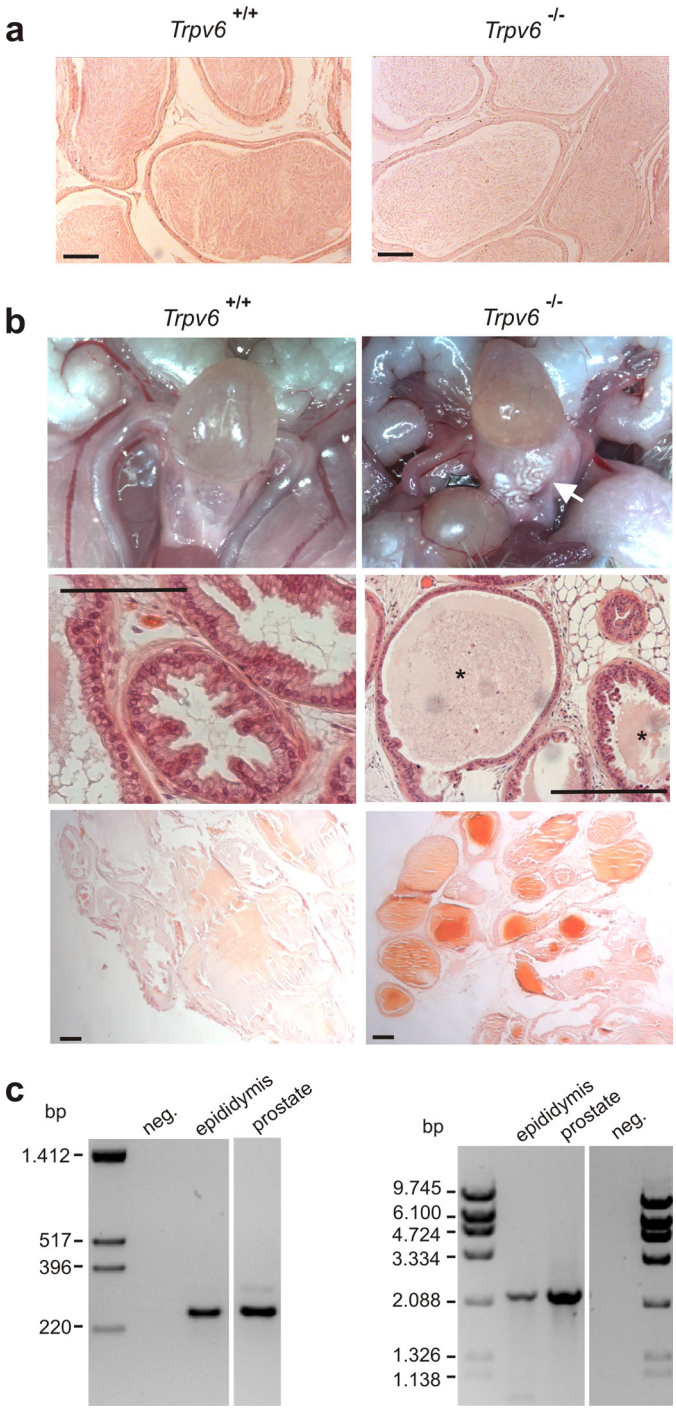

FIGURE 6. **Histological analysis of Ca^{2+} precipitations in epididymis and prostate.** *a*, alizarin red staining of the cauda epididymidis of wild-type and *Trpv6*$^{-/-}$ mice reveals no Ca^{2+} precipitations. *Scale bars*, 100 μm. *b*, whole mount images of the ventral and lateral lobes of the prostate from wild-type (*wt*) and *Trpv6*$^{-/-}$ mice (*upper*), hematoxylin/eosin-stained sections of the ventral lobe (*middle*), and alizarin red staining showing calcium deposition in the ventral lobe (*lower*). Ca^{2+} depositions (*upper panel*) are indicated as a *white arrow*. The loss of folding structures in the prostate ducts (*middle panel*) is marked by *asterisks*. *Scale bars*, 100 μm. *c*, amplification of a specific *Trpv6* cDNA fragment comprising 258 bp (*left*) and of full-length *Trpv6* cDNA comprising 2312 bp (*right*) from RNA of prostate and epididymis (as positive control) with reverse transcription-PCR. *neg.*, control reaction without RNA.

enlarged ducts of the ventral, dorsal, and lateral lobes of the prostate where *Trpv6* is also expressed in epithelial cells as in epididymal epithelial cells (1). As in *Trpv6*$^{D541A/D541A}$ mice, the

TABLE 1

Body weight analysis in male *Trpv6*$^{D541A/D541A}$ and *Trpv6*$^{-/-}$ mice

Body weight of mutant mice was normalized to their wild-type littermates; no significant difference was observed between *Trpv6*$^{D541A/D541A}$ and *Trpv6*$^{-/-}$ mice ($p > 0.05$) at all time points. The number of mutant and corresponding wild-type mice is indicated (*n*).

	Body weight							
	Wild type[a]		Male *Trpv6*$^{D541A/D541A}$		Male *Trpv6*$^{-/-}$		Wild type[b]	
Age	*n*	Normalized	*n*	Normalized	*n*	Normalized	*n*	Normalized
weeks		%		%		%		%
4	28	100	14	103 ± 4	9	97 ± 8	6	100
8	28	100	14	103 ± 2	9	100 ± 5	7	100
12	28	100	14	105 ± 2	9	99 ± 5	7	100
16	28	100	14	104 ± 2	9	105 ± 4	7	100

[a] The number of wild-type littermates of the group of *Trpv6*$^{D541A/D541A}$ mice.
[b] The number of wild-type littermates of the group of *Trpv6*$^{-/-}$ mice.

TABLE 2

Body weight analysis in female *Trpv6*$^{D541A/D541A}$ and *Trpv6*$^{-/-}$ mice

Body weight of mutant mice was normalized to their wild-type littermates; no significant difference was observed between *Trpv6*$^{D541A/D541A}$ and *Trpv6*$^{-/-}$ mice ($p > 0.05$) at all time points. The number of mutant and corresponding wild-type mice is indicated (*n*).

	Body weight							
	Wild type[a]		Female *Trpv6*$^{D541A/D541A}$		Female *Trpv6*$^{-/-}$		Wild type[b]	
Age	*n*	Normalized	*n*	Normalized	*n*	Normalized	*n*	Normalized
weeks		%		%		%		%
4	16	100	18	92 ± 4	6	102 ± 5	10	100
8	16	100	19	94 ± 2	7	103 ± 4	10	100
12	16	100	19	96 ± 3	7	96 ± 2	10	100
16	16	100	19	95 ± 2	7	97 ± 3	10	100

[a] The number of wild-type littermates of the group of *Trpv6*$^{D541A/D541A}$ mice.
[b] The number of wild-type littermates of the group of *Trpv6*$^{-/-}$ mice.

TABLE 3

Offspring analysis from matings with *Trpv6*$^{D541A/D541A}$ and *Trpv6*$^{-/-}$ males

No significant difference was observed between matings with *Trpv6*$^{D541A/D541A}$ and *Trpv6*$^{-/-}$ mice ($p > 0.05$). The number of matings for each setup is indicated (*n*). ND, not determined.

	Fertility rate					
Compared with			Male *Trpv6*$^{D541A/D541A}$ × female *Trpv6*$^{D541A/D541A}$		Male *Trpv6*$^{-/-}$ × female *Trpv6*$^{-/-}$	
Mating	*n*	%	*n*	%	*n*	%
Male *Trpv6*$^{+/D541A}$ × female *Trpv6*$^{D541A/D541A}$	11	100	7	1.29 ± 1.29		ND
Male *Trpv6*$^{+/-}$ × female *Trpv6*$^{-/-}$	5	100		ND	5	0.00 ± 0.00
Male *Trpv6*$^{+/+}$ × female *Trpv6*$^{+/+}$	8	100	7	1.25 ± 1.25	5	0.00 ± 0.00
Compared with			**Male *Trpv6*$^{D541A/D541A}$ × female *Trpv6*$^{+/D541A}$**		**Male *Trpv6*$^{-/-}$ × female *Trpv6*$^{+/-}$**	
Mating	***n***	**%**	***n***	**%**	***n***	**%**
Male *Trpv6*$^{+/D541A}$ × female *Trpv6*$^{D541A/D541A}$	11	100	7	1.94 ± 1.35		ND
Male *Trpv6*$^{+/-}$ × female *Trpv6*$^{-/-}$	5	100		ND	7	3.46 ± 1.85
Male *Trpv6*$^{+/+}$ × female *Trpv6*$^{+/+}$	8	100	7	1.87 ± 1.30	7	3.74 ± 2.00

TABLE 4

Analysis of copulatory behavior and *in vivo* fertilization rate

For analysis of copulatory behavior, the ratio of plug-positive wild-type females per mating with male *Trpv6*$^{D541A/D541A}$ and *Trpv6*$^{-/-}$ mice, respectively, was normalized to the ratio obtained from matings of wild-type females with wild-type males. Corresponding normalization was performed to compare the efficiency of *in vivo* fertilization assessed by microscopic analysis of flushed embryos from plug-positive wild-type females with males of the indicated genotype. No significant differences were observed between matings with *Trpv6*$^{D541A/D541A}$ and *Trpv6*$^{-/-}$ mice ($p > 0.05$). The number of matings for each experiment is indicated (*n*).

	Wild type		*Trpv6*$^{D541A/D541A}$		*Trpv6*$^{-/-}$	
Analysis of	*n*	%	*n*	%	*n*	%
Copulatory behavior	64	100	49	95.39 ± 17.21	120	114.57 ± 14.79
In vivo fertilization	15	100	11	2.75 ± 2,75	33	6.82 ± 5.69

Ca^{2+} deposits in the prostate cannot account for the massive elementary changes observed in caudal sperm of *Trpv6*$^{-/-}$ mice because these sperm are located upstream of the prostate and were never exposed to prostate secretions at this stage. Nevertheless, it cannot be fully excluded that cell-autonomous alterations in epithelial cells of the prostate contribute at least to some extent to the drastically reduced rate of offspring found in our mating analysis.

All functional deficits in the male reproductive tract that were found in *Trpv6*$^{-/-}$ mice are virtually identical to those we have found in *Trpv6*$^{D541A/D541A}$ mice and to those that have been described (1), suggesting that both the *Trpv6* gene excision (this study) and the specific D541A pore mutation (1) lead to a complete inactivation of TRPV6 channels. This conclusion is supported by a detailed comparison of the findings obtained with either mouse line. Development of body weight was not different between *Trpv6*$^{-/-}$ mice and *Trpv6*$^{D541A/D541A}$ mice (Tables 1 and 2). The fertility rate of homozygous mutant males (*Trpv6*$^{-/-}$ or *Trpv6*$^{D541A/D541A}$) was assessed in matings with either homozygous (*Trpv6*$^{-/-}$ and *Trpv6*$^{D541A/D541A}$) or heterozygous (*Trpv6*$^{+/-}$ and *Trpv6*$^{+/D541A}$) females and normalized to that obtained using *Trpv6*$^{+/D541A}$ or *Trpv6*$^{+/-}$ males, respectively. Apparently, the reduction in fertility rate

was not different between mice with either *Trpv6* mutation (Table 3). Also, no differences were observed in copulatory behavior or the rate of embryos isolated from plug-positive females of matings with males homozygous for either *Trpv6* mutation (Table 4). Motility parameters of caudal sperm were also reduced to the same extent, similar to the vitality of caudal sperm (Table 5); the only parameter in which we found a difference between sperm from $Trpv6^{-/-}$ and $Trpv6^{D541A/D541A}$ males was the overall motility, which could be due to an unusually high variability of this parameter in the group of $Trpv6^{-/-}$ mice. Concomitantly, the increase in Ca^{2+} concentration in the epididymal fluid and the reduction in Ca^{2+} uptake by the epididymal epithelium were identical in $Trpv6^{-/-}$ and $Trpv6^{D541A/D541A}$ males (Table 6). Such congruent functional deficits in $Trpv6^{-/-}$ mice and $Trpv6^{D541A/D541A}$ mice were not necessarily expected because $Trpv6^{D541A/D541A}$ mice, in contrast to $Trpv6^{-/-}$ mice, express TRPV6 proteins with an intact C terminus (Fig. 7) that contains binding sites for various proteins (19) including S100A10-annexin 2 (22), calmodulin (23), the PDZ protein Na^+/H^+ exchanger regulatory factor 4 (24), and Rab11a (25). These channel-associated proteins are hypothesized to integrate TRPV6 in the cytoskeletal network and to regulate the trafficking, anchoring, and activity of TRPV6 proteins at the plasma membrane, but it is unknown whether the thus formed protein complex has any additional functions. Whereas all these processes may work in $Trpv6^{D541A/D541A}$ mice, they cannot work in $Trpv6^{-/-}$ mice. Also, in other cation channels, such differences between mutations of the channel pore, even if they have profound effects on conductivity and permeability, and a complete loss of the corresponding channel protein are not unheard of. For instance, the G156S mutation in the pore-forming region of the Kir3.2 potassium channel causes a marked reduction of corresponding K^+ channels activated by G-protein-coupled receptors sim-

TABLE 5

Analysis of sperm motility and viability

Original data of different experiments in $Trpv6^{D541A/D541A}$ and $Trpv6^{-/-}$ mice were normalized to the corresponding wild type. No significant difference was observed between $Trpv6^{D541A/D541A}$ and $Trpv6^{-/-}$ mice ($p > 0.05$) except for overall motility. The number of analyzed animals is indicated (*n*). VAP, velocity, average path; VSL, velocity, straight line; VCL, velocity, curvilinear; IVF, *in vitro* fertilization.

	Wild type		$Trpv6^{D541A/D541A}$		$Trpv6^{-/-}$	
Analysis of sperm	*n*	%	*n*	%	*n*	%
Motility	6	100	6	7.32 ± 1.57	6	30.35 ± 9.55[a]
Progressive motility	6	100	6	6.18 ± 0.98	6	10.42 ± 6.33
VAP	6	100	6	68.26 ± 3.69	6	72.24 ± 5.63
VSL	6	100	6	83.06 ± 5.64	6	76.23 ± 4.29
VCL	6	100	6	64.09 ± 3.14	6	69.08 ± 5.51
IVF	5	100	5	14.47 ± 2.92	5	11.25 ± 4.43
Vitality caput	4	100	4	93.62 ± 1.36	4	95.84 ± 7.23
Vitality cauda	4	100	4	11.22 ± 2.32	4	22.20 ± 9.48

[a] $p = 0.04$.

TABLE 6

Comparison of defects in Ca^{2+} homeostasis in cauda epididymis of $Trpv6^{D541A/D541A}$ and $Trpv6^{-/-}$ mice

Absolute values of different experiments in $Trpv6^{D541A/D541A}$ and $Trpv6^{-/-}$ mice were normalized to the corresponding wild type and compared with each other. No significant difference between $Trpv6^{D541A/D541A}$ and $Trpv6^{-/-}$ mice was observed ($p > 0.05$).

	Wild type			$Trpv6^{D541A/D541A}$			$Trpv6^{-/-}$		
	n	[mM]	%	*n*	[mM]	%	*n*	[mM]	%
$[Ca^{2+}]_{out}$	29	0.19	100	28	1.9	1028	8	2.0	1123
Ca^{2+} uptake	16		100	16		13	10		11

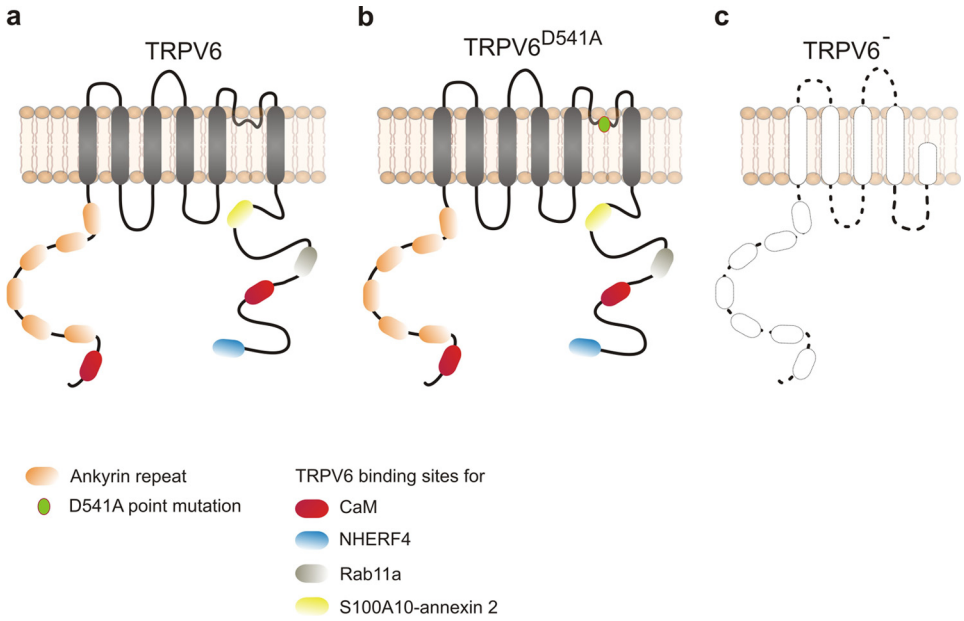

FIGURE 7. **Model of architecture of wild-type TRPV6 proteins, $TRPV6^{D541A}$ proteins, and potential proteins produced from the *Trpv6*-null ($Trpv6^{-}$) allele.** *a*, TRPV6 exhibits the typical topology of all members of the *transient receptor potential* family with six transmembrane regions and a short domain between transmembrane segments 5 and 6 forming the channel pore. The N-terminal region of wild-type TRPV6 contains at least five (possibly six) ankyrin repeats (5) and a binding site for calmodulin (*CaM*) (32). In the C-terminal tail of TRPV6, there are binding sites for calmodulin (23), Na^+/H^+ exchanger regulatory factor 4 (*NHERF4*) (24), Ras-related protein Rab-11A (*Rab11a*) (25), and S100A10-annexin 2 (22). *b*, replacement of aspartic acid at position 541 in the pore region of TRPV6 (Asp-541) eliminates Ca^{2+} conductivity of TRPV6 channels. This $TRPV6^{D541A}$ pore mutant protein is properly expressed and trafficked to the plasma membrane (1) and contains all binding sites for the TRPV6 interaction partners that anchor TRPV6 channel proteins in its native environment. *c*, proteins produced in cells homozygous for the *Trpv6*-null allele ($Trpv6^{-}$) lack part of transmembrane domain 5, the pore region, transmembrane domain 6, and the entire C-terminal tail due to the genetic ablation of exons 13, 14, and 15. Even if such truncated TRPV6 proteins are stable, the C-terminal binding sites for TRPV6-assocciated proteins are missing.

ilar to that in Kir3.2$^{-/-}$ mice (26, 27), whereas the spontaneous seizure activity observed in Kir3.2$^{-/-}$ mice is not evoked by the Kir3.2 G156S mutation. In another report, the Q618R mutation in the GluRδ2 channel pore that abrogates Ca^{2+} permeability rescues the deficits in synaptic plasticity of hippocampal neurons and motor coordination that were observed in GluRδ2$^{-/-}$ mice (20, 21). We found that the TRPV6 pore mutant (with an intact but non-functional protein still in place) led to very much the same phenotype as the deletion of almost one-third of the gene, which may lead to no TRPV6 protein expression at all or, if truncated proteins are formed, to a TRPV6 protein lacking 222 of 727 amino acid residues. Therefore, we conclude that the main function of TRPV6 proteins is their channel function and that even the persistence of the complete protein TRPV6^{D541A} does not contribute to functions that are absent in the *Trpv6*$^{-/-}$ mouse line.

In addition to the fertility analyses in the *Trpv6*$^{D541A/D541A}$ and *Trpv6*$^{-/-}$ mouse lines, there are also no differences in their gross appearance including growth. However, they differ significantly from a *Trpv6*-deficient mouse line generated by Bianco *et al.* (28). In this mouse line, the genomic sequences including exons 9–15 of the *Trpv6* gene as well as exons 15–18 of the adjacent *Ephb6* gene were deleted and replaced by a neomycin resistance cassette. In our *Trpv6*$^{-/-}$ mouse line, exons 17 and 18 of the *Ephb6* gene were deleted, whereas in the *Trpv6*$^{D541A/D541A}$ mouse line (1), all exons of the *Ephb6* gene were unchanged. Additionally, inactivation of *Ephb6* does not affect fertility as shown in two independent *Ephb6*$^{-/-}$ mouse lines (29, 30). The *Trpv6*$^{-/-}$ mice described by Bianco *et al.* (28) exhibit significant growth retardation, alopecia in 80% of all mice homozygous for the targeted allele, and impaired fertility in males but also in females (which was not characterized). Differences in growth, hair coat, or fertility of females were not observed in our *Trpv6*$^{-/-}$ or *Trpv6*$^{D541A/D541A}$ mice (this study and Ref. 1). The reason for the observed discrepancy with our *Trpv6*-deficient mouse line is not known, but differences may be due to deletion of either exons 15–18 of the *Ephb6* gene in *Trpv6*$^{-/-}$ mice described by Bianco *et al.* (28) or exons 17 and 18 in our mouse line. Additionally, disposition of the promotor-driven neomycin resistance cassette, which might affect expression of the adjacent *Trpv5* gene, or differences in the genetic background between the mouse lines cannot be excluded. The highly Ca^{2+}-selective TRPV5 channels resemble TRPV6 in many aspects as they are also constitutively active and exhibit many features possessed by Ca^{2+} transporters in epithelial cells (6, 7). TRPV5 plays a critical role in Ca^{2+} reabsorption in the kidney epithelium of collecting ducts, but *Trpv5*$^{-/-}$ mice show no defect in fertility (31). Obviously, the defect in Ca^{2+} uptake in the epididymal epithelium induced by deletion of the *Trpv6* gene could not be compensated for by the nearest relative, TRPV5, demonstrating that TRPV6 is essential for the posttesticular sperm maturation process.

In summary, we demonstrated that *Trpv6*$^{-/-}$ mice show phenotypic changes in the male reproductive tract equal to those in *Trpv6*$^{D541A/D541A}$ mice, corroborating the crucial role of TRPV6 in the epididymis for the development of fertilization capacity of sperm. We conclude that TRPV6 proteins are essential components of Ca^{2+}-conducting channel complexes in the apical membrane of epididymal epithelial cells and are responsible for decreasing the Ca^{2+} concentration of the intraluminal fluid in the cauda epididymis. Furthermore, the results obtained with the *Trpv6*$^{-/-}$ mice underscore the finding in *Trpv6*$^{D541A/D541A}$ mice that appropriate regulation of intraluminal Ca^{2+} concentration in the epididymal duct is essential for the production of fertilization-ready spermatozoa during the epididymal passage. Together with the phenotype analysis of *Trpv6*$^{D541A/D541A}$ mice, our results argue for the conclusion that the D541A pore mutation leads to a complete inactivation of TRPV6 channels in the epididymal epithelium.

Acknowledgments—We thank S. Buchholz, C. Matka, T. Volz, K. Fischer, S. Schmidt, and S. Tasch for expert technical assistance.

REFERENCES

1. Weissgerber, P., Kriebs, U., Tsvilovskyy, V., Olausson, J., Kretz, O., Stoerger, C., Vennekens, R., Wissenbach, U., Middendorff, R., Flockerzi, V., and Freichel, M. (2011) Male fertility depends on Ca^{2+} absorption by TRPV6 in epididymal epithelia. *Sci. Signal.* **4,** ra27
2. Hoenderop, J. G., van der Kemp, A. W., Hartog, A., van de Graaf, S. F., van Os, C. H., Willems, P. H., and Bindels, R. J. (1999) Molecular identification of the apical Ca^{2+} channel in 1,25-dihydroxyvitamin D_3-responsive epithelia. *J. Biol. Chem.* **274,** 8375–8378
3. Peng, J. B., Chen, X. Z., Berger, U. V., Vassilev, P. M., Tsukaguchi, H., Brown, E. M., and Hediger, M. A. (1999) Molecular cloning and characterization of a channel-like transporter mediating intestinal calcium absorption. *J. Biol. Chem.* **274,** 22739–22746
4. Hirnet, D., Olausson, J., Fecher-Trost, C., Bödding, M., Nastainczyk, W., Wissenbach, U., Flockerzi, V., and Freichel, M. (2003) The TRPV6 gene, cDNA and protein. *Cell Calcium* **33,** 509–518
5. Wissenbach, U., Niemeyer, B. A., Fixemer, T., Schneidewind, A., Trost, C., Cavalie, A., Reus, K., Meese, E., Bonkhoff, H., and Flockerzi, V. (2001) Expression of CaT-like, a novel calcium-selective channel, correlates with the malignancy of prostate cancer. *J. Biol. Chem.* **276,** 19461–19468
6. Hoenderop, J. G., Nilius, B., and Bindels, R. J. (2003) Epithelial calcium channels: from identification to function and regulation. *Pflugers Arch.* **446,** 304–308
7. Peng, J. B., Brown, E. M., and Hediger, M. A. (2003) Epithelial Ca^{2+} entry channels: transcellular Ca^{2+} transport and beyond. *J. Physiol.* **551,** 729–740
8. Vennekens, R., Hoenderop, J. G., Prenen, J., Stuiver, M., Willems, P. H., Droogmans, G., Nilius, B., and Bindels, R. J. (2000) Permeation and gating properties of the novel epithelial Ca^{2+} channel. *J. Biol. Chem.* **275,** 3963–3969
9. Voets, T., Janssens, A., Prenen, J., Droogmans, G., and Nilius, B. (2003) Mg^{2+}-dependent gating and strong inward rectification of the cation channel TRPV6. *J. Gen. Physiol.* **121,** 245–260
10. Darszon, A., Acevedo, J. J., Galindo, B. E., Hernández-González, E. O., Nishigaki, T., Treviño, C. L., Wood, C., and Beltrán, C. (2006) Sperm channel diversity and functional multiplicity. *Reproduction* **131,** 977–988
11. Evans, J. P., and Florman, H. M. (2002) The state of the union: the *cell* biology of fertilization. *Nat. Cell Biol.* **4,** (suppl.) s57–s63
12. Levine, N., and Kelly, H. (1978) Measurement of pH in the rat epididymis *in vivo*. *J. Reprod. Fertil.* **52,** 333–335
13. Acott, T. S., and Carr, D. W. (1984) Inhibition of bovine spermatozoa by caudal epididymal fluid: II. Interaction of pH and a quiescence factor. *Biol. Reprod.* **30,** 926–935
14. Jenkins, A. D., Lechene, C. P., and Howards, S. S. (1980) Concentrations of seven elements in the intraluminal fluids of the rat seminiferous tubules, rate testis, and epididymis. *Biol. Reprod.* **23,** 981–987
15. Turner, T. T. (1991) Spermatozoa are exposed to a complex microenvironment as they traverse the epididymis. *Ann. N.Y. Acad. Sci.* **637,** 364–383

16. Levine, N., and Marsh, D. J. (1971) Micropuncture studies of the electrochemical aspects of fluid and electrolyte transport in individual seminiferous tubules, the epididymis and the vas deferens in rats. *J. Physiol.* **213,** 557–570
17. Freichel, M., Wissenbach, U., Philipp, S., and Flockerzi, V. (1998) Alternative splicing and tissue specific expression of the 5′ truncated bCCE 1 variant bCCE 1Δ514. *FEBS Lett.* **422,** 354–358
18. Farley, F. W., Soriano, P., Steffen, L. S., and Dymecki, S. M. (2000) Widespread recombinase expression using FLPeR (flipper) mice. *Genesis* **28,** 106–110
19. van de Graaf, S. F., Hoenderop, J. G., and Bindels, R. J. (2006) Regulation of TRPV5 and TRPV6 by associated proteins. *Am. J. Physiol. Renal. Physiol.* **290,** F1295–F1302
20. Wollmuth, L. P., Kuner, T., Jatzke, C., Seeburg, P. H., Heintz, N., and Zuo, J. (2000) The Lurcher mutation identifies δ2 as an AMPA/kainate receptor-like channel that is potentiated by Ca^{2+}. *J. Neurosci.* **20,** 5973–5980
21. Kakegawa, W., Miyazaki, T., Hirai, H., Motohashi, J., Mishina, M., Watanabe, M., and Yuzaki, M. (2007) Ca^{2+} permeability of the channel pore is not essential for the δ2 glutamate receptor to regulate synaptic plasticity and motor coordination. *J. Physiol.* **579,** 729–735
22. van de Graaf, S. F., Hoenderop, J. G., Gkika, D., Lamers, D., Prenen, J., Rescher, U., Gerke, V., Staub, O., Nilius, B., and Bindels, R. J. (2003) Functional expression of the epithelial Ca^{2+} channels (TRPV5 and TRPV6) requires association of the S100A10-annexin 2 complex. *EMBO J.* **22,** 1478–1487
23. Niemeyer, B. A., Bergs, C., Wissenbach, U., Flockerzi, V., and Trost, C. (2001) Competitive regulation of CaT-like-mediated Ca^{2+} entry by protein kinase C and calmodulin. *Proc. Natl. Acad. Sci. U.S.A.* **98,** 3600–3605
24. van de Graaf, S. F., Hoenderop, J. G., van der Kemp, A. W., Gisler, S. M., and Bindels, R. J. (2006) Interaction of the epithelial Ca^{2+} channels TRPV5 and TRPV6 with the intestine- and kidney-enriched PDZ protein NHERF4. *Pflugers Arch.* **452,** 407–417
25. van de Graaf, S. F., Chang, Q., Mensenkamp, A. R., Hoenderop, J. G., and Bindels, R. J. (2006) Direct interaction with Rab11a targets the epithelial Ca^{2+} channels TRPV5 and TRPV6 to the plasma membrane. *Mol. Cell. Biol.* **26,** 303–312
26. Jarolimek, W., Bäurle, J., and Misgeld, U. (1998) Pore mutation in a G-protein-gated inwardly rectifying K^+ channel subunit causes loss of K^+-dependent inhibition in weaver hippocampus. *J. Neurosci.* **18,** 4001–4007
27. Lüscher, C., Jan, L. Y., Stoffel, M., Malenka, R. C., and Nicoll, R. A. (1997) G protein-coupled inwardly rectifying K^+ channels (GIRKs) mediate postsynaptic but not presynaptic transmitter actions in hippocampal neurons. *Neuron* **19,** 687–695
28. Bianco, S. D., Peng, J. B., Takanaga, H., Suzuki, Y., Crescenzi, A., Kos, C. H., Zhuang, L., Freeman, M. R., Gouveia, C. H., Wu, J., Luo, H., Mauro, T., Brown, E. M., and Hediger, M. A. (2007) Marked disturbance of calcium homeostasis in mice with targeted disruption of the Trpv6 calcium channel gene. *J. Bone Miner. Res.* **22,** 274–285
29. Luo, H., Yu, G., Tremblay, J., and Wu, J. (2004) EphB6-null mutation results in compromised T cell function. *J. Clin. Investig.* **114,** 1762–1773
30. Shimoyama, M., Matsuoka, H., Nagata, A., Iwata, N., Tamekane, A., Okamura, A., Gomyo, H., Ito, M., Jishage, K., Kamada, N., Suzuki, H., Tetsuo Noda, T., and Matsui, T. (2002) Developmental expression of EphB6 in the thymus: lessons from EphB6 knockout mice. *Biochem. Biophys. Res. Commun.* **298,** 87–94
31. Hoenderop, J. G., van Leeuwen, J. P., van der Eerden, B. C., Kersten, F. F., van der Kemp, A. W., Mérillat, A. M., Waarsing, J. H., Rossier, B. C., Vallon, V., Hummler, E., and Bindels, R. J. (2003) Renal Ca^{2+} wasting, hyperabsorption, and reduced bone thickness in mice lacking TRPV5. *J. Clin. Investig.* **112,** 1906–1914
32. Lambers, T. T., Weidema, A. F., Nilius, B., Hoenderop, J. G., and Bindels, R. J. (2004) Regulation of the mouse epithelial Ca^{2+} channel TRPV6 by the Ca^{2+}-sensor calmodulin. *J. Biol. Chem.* **279,** 28855–28861